International Journal for Housing Science and Its Applications
Publish September 8, 2025. Volume 47, Issue 1 Pages 146-152

https://doi.org/10.70517/ijhsa47112

Biological mechanisms of children's social skill development based on self-attentive adversarial deep subspace clustering

Sisi Zhao
International Education College, Wuchang Institute of Technology, Wuhan 430065, Hubei, China; season202401@163.com).

Abstract This study investigates the biological processes that support children's social skill development in the framework of familial interactions. The study looks at multidimensional datasets, such as physiological biomarkers, brain activity, and observed behaviors, using a attentive adversarial deep subspace clustering (SAADSC) algorithm to find patterns that connect competences to family dynamics. The results show that brain configurations that support social functioning are consistently linked to high levels of family cohesion. Furthermore, the accuracy of behavioral outcome predictions is significreased by include physiological factors in the analytical model, such as heart rate variability and cortisol concentration. Through a data-driven, interdisciplinary lens, this integrated methodology provides important insights for developmental psychology and social neuroscience by revealing how biological systems moderate environmental impacts.

Index Terms self-attentive adversarial deep subspace clustering, family function, biological indicator integration

I. Introduction

Children's social skill development is a complex process influenced by a combination of biological, environmental, and genetic factors [1], [2]. The foundation of these is family function, which affects interpersonal communication, emotional control, and general social interaction. In order to comprehend how biological markers—such as hormone levels, brain activity, and physe social behavior, research has recently placed a greater emphasis on this relationship [3], [4]. However, there remains a critical need for comprehensive models that integrate these diverse elements to provide deeper insights into children's social skill development. This study aims to bridge this gap by incorporating biological and behavioral data, utilizing the SAADSC (Social-Behavioral and Adaptive Developmental System Classification) framework [5], [6].

By leveraging neural networks and advanced computational techniques, this research investigates the intricate relationships between family environments and biological indicators, including cortisol levels, heart rate variability, and other neurobiological signals [7]. Neural networks, known for their capacity to identify and model complex patterns, enable the detailed analysis of how these biological factors interact with environmental influences, such as family cohesion, parental support, and stress levels [8]–[10]. The inclusion of biological behavioravous system activity, provides valuable insights into the physiological mechanisms underpinning social skill acquisition [11], [12]. These biomarkers offer a quantifiable means to assess emotional and social processing, which can be critical for identifying children at risk of social development delays.

This study adopts a multidisciplinary approach that integrates developmental biology, neuroscience, and advanced computational modeling to explore the interplay between biological and environmental factors. Through the SAADSC framework, we examine the dynamic interactions that influence social competence, emphasizing how family function modulates neurobiological responses to social stimuli. For instance, supportive family environments are linked to stotional regulation and social adaptability. Conversely, dysfunctional family dynamics are associated with dysregulated stress responses and impaired neural activity, which can hinder social skill development.

Furthermore, this study advances the field by providing useful implications for interventions meant to enhance children's social outcomes. Targeted solutions to support children in difficult family circumstances can be devised by identifying important biological indicators linked to social competence. Future research avenues include developing neural network models ttent of biological data integration, including the incorporation of genetic and epigenetic elements. This all-encompassing strategy not only improves our knowledge of child development but also opens the door for cutting-edge approaches in social neuroscience and developmental science.

II. Methods

II. A. Integration of biomechanical data

A greater comprehension of the relationship between children's social development and physiological and physical factors can be gained by integrating biomechanical principles into the analysis framework. An important viewpoint on how biological processes impact behavior is offered by biomechanics, which studies the mechanical rules pertaining to the motion and composition of living things [12], [13]. In order to investigate the physical foundations of brain and behavioral connections in the development of social skills, we incorporated biomechanical data into the self-attentive adversarial deep subspace clustering (SAADSC) model.

Here's a refined approach to enhancing the methodology section based on the given content:

Data Preprocessing: Describe how biomechanical and neurobiological data are preprocessed before being incorporated into the SAADSC model. For example, explain any techniques utilized for noise reduction, dimensionality reduction, or normalization.Model Initialization: Indicate the SAADSC model's starting parameter values, including the convolutional network's layer count, channel sizes, and kernel dimensions.Feature Extraction: Describe the computational procedure used to create the attention map as well as how the self-attention module handles input data to produce K, Q, and V matrices.

Parameter selection

Channel Count and Attention Modules: Provide evidence justifying the inclusion of the residual module for deep feature learning and the use of 1000 channels in the penultimate layer. Talk about any empirical studies or earlier research that backed up these decisions. Gradient Penalty Coefficient: To guarantee Lipschitz continuity and discriminator stability, explain why the particular gradient penalty coefficient utilized in WGAN-GP or WGAN-div is chosen. Residual Module Kernel Size and Step Size: Describe the selection of 3×3 kernels with a step size of 1 and highlight how they affect network performance and feature extraction depth.

Model training and verification

Describe the dataset split (e.g., training, validation, and testing sets) and the criteria used for partitioning (e.g., stratified sampling). Specify the number of training epochs, batch sizes, and learning rate schedules used during training.Enumerate metrics (e.g., clustering accuracy, normalized mutual information, and silhouette scores) used to evaluate the model's clustering and generative performancePerform ablation studies to measure the impact of the self-attention module and residual connections on performance.

By adding these details, the methodology section will provide a comprehensive and transparent explanation of the implemented techniques, ensuring reproducibility and clarity for the readers.

The self-attentive adversarial deep subspace clustering (SAADSC) network's architecture is shown in Figure 1. A self-attention module is incorporated into the encoder module's last convolutional network layer to guarantee long-range dependency in feature learning. Figure 2 further illustrates the self-attention module's design and functional aspects.

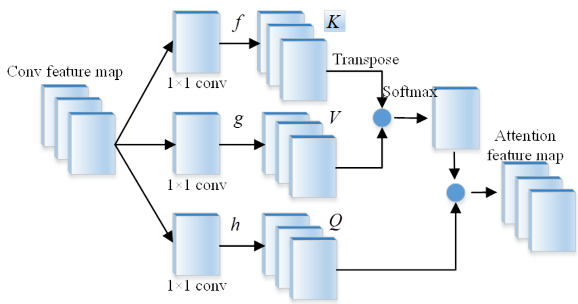

Figure 1: Module for self-attention

This module creates the key (K), query (Q), and value (V) matrices by performing a 1×1 convolution operation on the data output from the network's previous layer. First, the self-attention mechanism multiplies the value (V) by the dot product of the query (Q) and the transposed key (K). The final self-attention feature map is obtained by normalizing this procedure using a softmax function. By efficiently capturing feature interdependencies, this method improves the network's capacity to learn more resilient and discriminative feature representations [14].

In the training of generative adversarial networks (GANs), when the discriminator becomes excessively dominant, it often results in vanishing gradients, thereby obstructing effective generator updates. To address this, many scholars have proposed improvements to the loss function. Traditional cross-entropy-based divergence metrics—such as Kullback-Leibler (KL) or Jensen-Shannon (JS) divergence—suffer from limitations, especially when the real and generated data distributions do not significantly overlap. As shown in Eq. (1), these approaches are highly sensitive to the support of the distributions, which often leads to training instability.

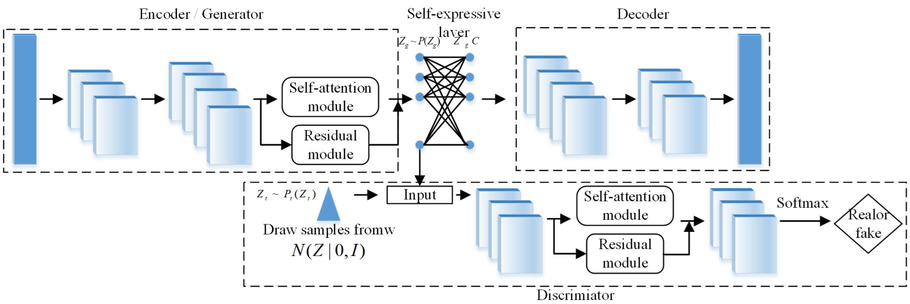

Figure 2: Self-attention confrontation-based deep subspace clustering network framework

To mitigate this problem, the Wasserstein Generative Adversarial Network (WGAN) introduces a new objective function based on the Earth Mover's (EM) distance, also known as the Wasserstein-1 distance. This metric provides a more meaningful and smoother gradient even when distributions lie on low-dimensional manifolds.

The WGAN modifies the loss formulation as follows:

Discriminator (Critic) loss:

$$L_D = \mathbb{E}_{x\sim P_r}[D(x)] - \mathbb{E}_{\tilde{x}\sim P_g}[D(\tilde{x})]. \tag{1}$$

Generator loss:

$$L_G = -\mathbb{E}_{\tilde{x}\sim P_g}[D(\tilde{x})]. \tag{2}$$

Here, P_r denotes the real data distribution, and P_g represents the generator's data distribution. Unlike cross-entropy, this formulation eliminates logarithmic terms and instead focuses on measuring the minimal effort required to transform one distribution into another.

Through this refined metric, WGAN effectively stabilizes the adversarial training process, reduces mode collapse, and offers more consistent gradients for generator updates—even when the discriminator is close to optimal. (see Figure 1–2).

The loss function of our network's generative adversarial network component is built by combining the GAN and its variations that were previously researched.

$$\mathcal{L}_{dis} = E_{Z_g\sim P_g(Z_g)}\left[f_D\left(Z_g\right)\right] - E_{Z_r\sim P_r(Z_r)}\left[f_D\left(Z_r\right)\right] + \lambda_3 E_{\hat{Z}\sim P(\hat{Z})}\left[\left\|f_D(\nabla\hat{Z})\right\|^3\right]. \tag{3}$$

In generative adversarial networks, the generative element that generates feature representations is the coding module. According to the structure of the generative adversarial network, B represents the false samples, while the genuine samples are taken from the prior distribution, which is usually a conventional Gaussian distribution, a mixed Gaussian distribution, etc. [14]. The generator's feature distribution gradually approaches the preset prior distribution structure through game training after the true and false samples are combined and supplied into the discriminator. The samples, which are then used as observational data to improve the network's anti-interference capabilities and the resilience of feature learning, are generated by the decoder using the prior distribution p(z) [15]. By applying a gradient penalty to stabilize the output of gradient information, the discriminator guarantees the stability of the generator update. This framework is used to rewrite Eq. (3) as follows:

$$\mathcal{L}_c = \frac{1}{2}X - \hat{X}_F^2 + \frac{\lambda_1}{2}\left\|Z_g - Z_g C\right\|_F^2 + \lambda_2 C_F\ . \tag{4}$$

To enhance feature representation, we introduce an adversarial network with structural characteristics that resemble a prior distribution, improving the performance of the network beyond the capabilities of Eq. (3). This modification significantly refines the way the model learns complex data representations. Furthermore, we incorporate a residual module into the white attention module, which contributes to increasing the network depth and facilitates the learning of more abstract feature representations.

Since the residual module is completely integrated into the architecture, its inclusion has no effect on the deep neural network's loss function. The output of the self-attention module and the residual module are merged, and the resulting output is then sent as input into the neural network's next layer. This method allows for more effective training by improving feature propagation and avoiding the vanishing gradient issue that frequently arises in deeper networks.

The residual module is equipped with two convolutional kernels of size 3×3 and a stride of 1. These kernels are designed to capture fine-grained spatial features within the data while maintaining the network's computational efficiency. By stacking multiple residual blocks, the network is able to learn increasingly sophisticated features without significantly increasing computational complexity.

II. B. Biomechanical Data Acquisition

To complement neurobiological and hormonal indicators, we collected data on motor coordination, posture, and movement patterns, as these aspects are closely tied to social interactions [16]. The biomechanical measurements included:

Evaluating the symmetry and rhythm of walking, which reflects motor control and can indirectly indicate social anxiety or confidence levels.

Using force plates to measure the center of pressure (CoP) displacement during static and dynamic conditions. Postural control is essential for non-verbal communication, such as maintaining eye contact.

Assessing kinematic variables during task performance to understand the precision and fluidity of actions, often linked to social competence in group settings.

When generative adversarial methods and clustering are combined, the network's overall loss function is:

$$\mathcal{L}_{total} = \mathcal{L}_c + \mathcal{L}_{gen} + \mathcal{L}_{dis} . \tag{5}$$

A generative adversarial network is trained by iteratively training the discriminative loss and the generating loss, which leads to mutual updating. Repeat steps 1–3 until the maximum epoch value is reached. After network training is complete, the nearby relationship of the data will be learned, and the clustering result of the data is obtained by grouping the output self-representation coefficient c using spectral clustering.

II. C. Biomechanical feature integration

The high-dimensional biomechanical data were processed through the SAADSC framework to ensure effective clustering and representation. Key steps included:

All biomechanical variables were normalized to account for inter-individual differences in body size and movement patterns [17].

Biomechanical data were fused with neurobiological and hormonal signals using a self-attention mechanism. This integration allowed the model to capture complex interdependencies between movement dynamics and social behaviors.

Given that biomechanics involves time-sensitive processes, temporal convolutional layers were added to the network to extract time-series patterns. This enabled the model to identify how changes in movement corresponded to shifts in social engagement or stress levels.

To verify the effectiveness of the proposed algorithm, this study conducted experiments on five public datasets, including two handwritten digit datasets (MNIST and USPS), an object recognition dataset (COIL-20), a facial recognition dataset (Extended Yale B, hereinafter referred to as Yale B), and a clothing image dataset (Fashion MNIST, hereinafter referred to as FMNIST). The experimental environment includes an Ubuntu system configured with CUDA 8.0 and cuDNN 5.1, the hardware uses four NVIDIA GTX 1080Ti graphics cards, the main deep learning framework is TensorFlow 1.0, and Python language is used for modeling and simulation. During the experiment, we set the input weight parameters. Among them, the control parameters of the self-expression term and the regularization term are Inputs 1 and A2 respectively, and Inputs 1 is set to 1 to simplify the parameter adjustment process. In addition, to improve the stability of the model, the gradient penalty term in the generative adversarial network is introduced to reduce the influence of the parameters in formula (5) on the experimental results [18]. The following Table 1-2 lists the basic information of each dataset used in the experiment:

Table 1: Dataset descriptions

Dataset name	Number of classes	Samples per class	Image size	Data type
MNIST	10	7000	28×28	Handwritten digits
USPS	10	1100	16×16	Handwritten digits
COIL-20	20	72	32×32	Object images
Yale B	38	64	32×32	Facial images
Fashion MNIST	10	7000	28×28	Clothing images

Table 2: Experimental parameter settings

Parameter name	Value	Description
Inputs 1	1	Weight parameter for self-representation
A2	0.1	Weight parameter for regularization term
Batch Size	256	Number of samples per training iteration
Learning Rate	0.0002	Learning rate for the optimizer
Optimizer	Adam	Algorithm used for weight updates
Number of Epochs	200	Total number of training iterations
Discriminator Update Freq	5	Discriminator updates every 5 generator iterations

III. Result

Both the encoder and the decoder are symmetric in the experiments, and the encoder has a three-layer convolutional network topology.A single-layer convolutional network and three residual modules make up Fashion-MNIST's encoder, while the decoder also has a symmetric layout. Table 3 lists the precise parameters of the single-layer convolutional network that COIL-20 utilizes.

Table 3: Parameters of the single-layer convolutional network in the COIL-20 decoder

Layer	Layer type	Kernel size	Stride	Padding	Activation function	Output channels
Layer 1	Deconvolution	5×5	2	SAME	ReLU	64
Layer 2	Deconvolution	5×5	2	SAME	ReLU	128
Layer 3	Deconvolution	5×5	1	SAME	ReLU	256
Output	Convolution	3×3	1	SAME	Sigmoid	3

To improve the information sharing across channels, the discriminator network uses a three-layer 1×1 convolutional network in each experiment. The number of channels is 1000, 1000, and 11, respectively.To improve the long-range reliance of the 1000 channel characteristics, a self-attention module is also added to the discriminator network's penultimate layer. Traditional deep clustering methods typically use a self-encoder to do the algorithm's pre-training. However, because this paper's technique uses a generative adversarial network, we decided to employ the adversarial auto-encoder (AAE) for pre-training to prevent the discriminator's initial training from being too strong to obstruct feature learning [19].

III. A. Indicators of evaluation

We employ two widely used metrics to assess our algorithm's superiority: Standard Mutual Information (NMI), which measures the clustering effect.

$$NMI\% = \frac{2I(A,B)}{H(A)+H(B)} \times 100\%. \tag{6}$$

We chose several deep clustering techniques, such as Struct-AE1521, DASC, DCN, DSC, and DEC, that are associated with the suggested algorithm for comparison in our studies. The experimental outcomes are compiled in Table 4. The best outcomes are displayed in bold, and the experimental data are averaged over 30 trials. The experimental data for Struct-AE and DASC are taken from the original articles because their codes are not publicly available. Furthermore, these two approaches were not compared because they were not evaluated on the FMNIST and USPS datasets. While we test the experimental results of FMNIST and USPS, the experimental results of DSC and MNIST are cited in the original works for the Yale B and COIL-20 datasets.The remaining data comes from the original studies, and we test the experimental results of DEC and DCN on Yale B vs. COIL-20. It should be mentioned that DEC's test results on Yale B are not reported and are given the designation "B" because the findings are not realistic and do not significantly improve even after changing the parameters multiple times [20].

Table 4 shows that the suggested algorithm performs better than the other six approaches in terms of both ACC and NMI measures. For instance, when compared to the next best DEC, our algorithm improves the ACC by 0.1110 and the NMI by 0.1281 on the MNIST dataset. In contrast, the DEC results on Yale B and the DCN on COIL-20 perform poorly, primarily due to their inability to adequately capture the correlation between data due to their lack of self-representation structure. On some of the data, however, DSC, DASC, and the techniques in this paper that use self-representation structure outperform the others.

We visualize the MNIST training loss in order to evaluate the stability of the suggested generative adversarial network. By adding the self-attention module and the adversarial mechanism, this network considerably increases the clustering accuracy and NMI when compared to DSC-L2.Furthermore, we use three distinct distributions on three datasets for comparative experiments to investigate the effects of various prior distributions on the experimental outcomes, which further confirms the algorithm's superiority.

Table 4: Five datasets' experimental results

Data set	Yale B		COIL-20		MNIST		FMNIST		USPS	
Measurement method	ACC	NMI	ACC	NMI	ACC	NMI	ACC	NMI	ACC	NMI
DSC-L1	0.9666	0.9685	0.9316	0.9393	0.7283	0.7215	0.4768	0.6153	0.6985	0.6767
DSC-L2	0.9735	0.9701	0.9366	0.9405	0.7503	0.7316	0.5816	0.6135	0.7286	0.6965
DEC	*	*	0.6286	0.7788	0.8433	0.8000	0.5903	0.6013	0.7526	0.7406
DCE	0.4303	0.6303	0.1888	0.3036	0.7505	0.7485	0.5866	0.5941	0.7382	0.7692
Struct-AE	0.9722	0.9736	0.9325	0.9563	0.6572	0.6999	-	-	-	-
DASC	0.9855	0.9803	0.9637	0.9585	0.8043	0.7803	-	-	-	-
SAADSC	0.9898	0.9853	0.9752	0.9747	0.9544	0.9283	0.6316	0.6245	0.7853	0.8136

We created a number of independent tests to assess each module's function inside the suggested network: Test 1 shows the network after the self-attention and residual modules have been removed; Test 2 shows the network after the self-representation layer has been removed and the adjacency matrix created by (c = alpha) has been clustered using the spectral clustering algorithm; Test 3 also removes the self-representation layer but substitutes K-means clustering for B; and Test 4 shows the network after the residual module has been removed.

The findings indicate that the self-representation layer has the biggest influence on network performance, followed by the self-attention module, while the residual module has the least improvement. By creating linear representations for the data between them, the self-representation layer produces coefficient matrices that can accurately depict both the independence of the data between classes and the correlation of the data within classes. This results in a notable improvement in network performance(see Figure 3).

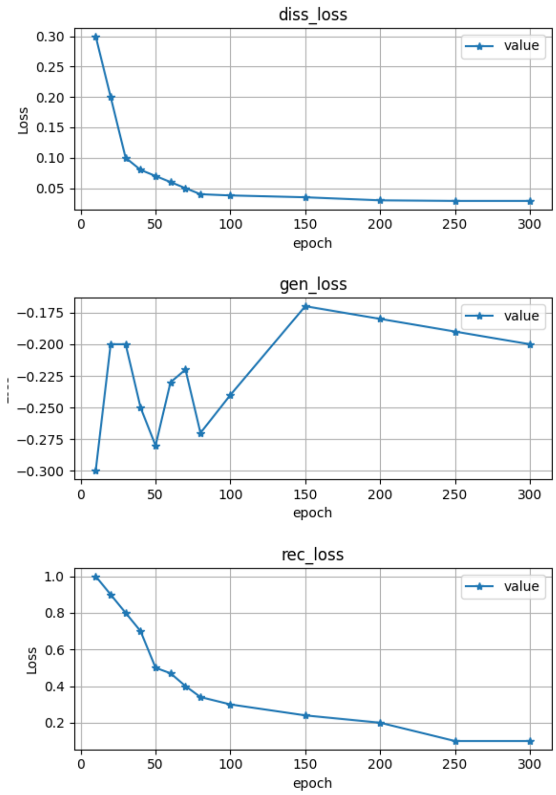

Figure 3: Training loss curve of the network on MNIST dataset

IV. Conclusion

This study shows how well the SAADSC framework works for examining intricate correlations in a variety of datasets, especially when it comes to kids' social skill development. The SAADSC model demonstrated its capacity to identify complex patterns in biological markers, including cortisol levels, heart rate variability, and neural activation, by fusing neural networks with biological behavioral data. These results demonstrate how well the algorithm performs in deep clustering tasks, allowing for a more nuanced comprehension of the interaction between environmental and biological elements.The results confirm that the self-attentive adversarial deep subspace clustering framework excels in handling high-dimensional, multimodal datasets by leveraging its self-attention modules and robust adversarial training mechanisms. The model demonstrated resilience to noise and improved feature representation through the integration of gradient penalties and residual connections, leading to superior clustering accuracy compared to traditional approaches.

References

[1] Wakimizu, R. , & Wang, T. . (2022). Parenting stress of chinese mothers living and child-rearing in japan and related factors. *Journal of Nursing (English), 12*(2), 18

[2] Schuler, B. R. , Daundasekara, S. S. , Hernandez, D. C. , Dumenci, L. , & Miller, A. L. . (2020). Economic hardship and child intake of foods high in saturated fats and added sugars: the mediating role of parenting stress among high-risk families. *Public Health Nutrition, 23*(15), 1-12.

[3] Schreiber, J. E., Cole, J. C., Houtrow, A. J., Kallan, M. J., Thom, E. A., Howell, L. J., & Adzick, N. S. (2021). Maternal depressive risk in prenatal versus postnatal surgical closure of myelomeningocele: associations with parenting stress and child outcomes. Fetal Diagnosis and Therapy, 48(6), 479-484.

[4] Maughan, A. L., Lunsky, Y., Lake, J., Mills, J. S., Fung, K., Steel, L., & Weiss, J. A. (2024). Parent, child, and family outcomes following Acceptance And Commitment Therapy for parents of autistic children: A randomized controlled trial. *Autism, 28*(2), 367-380.

[5] Haque, M. A., Salwa, M., Sultana, S., Tasnim, A., Towhid, M. I. I., Karim, M. R., & Abdullah Al Mamun, M. (2022). Parenting stress among caregivers of children with neurodevelopmental disorders: a cross-sectional study in bangladesh:. *Journal of Intellectual Disabilities, 26*(2), 407-419.

[6] Ji, Y. L. , & Lee, K. . (2021). Effects of parenting stress on preschoolers' emotion regulation: mediating role of parent's responses to children's negative emotions. *Korean Journal of Child Studies, 42*(1), 119-134.

[7] Wiley, B. , Ghanim, F. , Taylor, K. , & Murias, K. . (2021). P.124 baseline assessment of attention and executive function deficits in children with neurodevelopmental disorders: data from a speciality attention clinic. *Canadian Journal of Neurological Sciences / Journal Canadien des Sciences Neurologiques, 48*(s3), S54-S55.

[8] Park, M. N., Moulton, E. E., & Laugeson, E. A. (2023). Parent-assisted social skills training for children with autism spectrum disorder: PEERS for preschoolers. *Focus on Autism and Other Developmental Disabilities, 38*(2), 80-89.

[9] Wolf, J. P. , Freisthler, B. , & Chadwick, C. . (2021). Stress, alcohol use, and punitive parenting during the covid-19 pandemic. *Child Abuse & Neglect, 117*(5), 105090.

[10] Shin, E. , Choi, K. , Resor, J. , & Smith, C. L. . (2021). Why do parents use screen media with toddlers? the role of child temperament and parenting stress in early screen use. *Infant Behavior and Development, 64*(5), 101595.

[11] Falb, K. L., Asghar, K., Blackwell, A., Baseme, S., Nyanguba, M., Roth, D., & de Dieu Hategekimana, J. (2023). Improving family functioning and reducing violence in the home in North Kivu, Democratic Republic of Congo: a pilot cluster-randomised controlled trial of Safe at Home. BMJ open, 13(3), e065759.

[12] Cheng, A. W., & Lai, C. Y. (2023). Parental stress in families of children with special educational needs: a systematic review. *Frontiers in Psychiatry, 14*, 1198302.

[13] Tolosana, N., Carrera, M., de Villoria, R. G., Castejon, L., & Miravete, A. (2012). Numerical analysis of three-dimensional braided composite by means of geometrical modeling based on machine emulation. Mechanics of Advanced Materials and Structures, 19(1-3), 207-215.

[14] Feather, J., Leclerc, G., Mądry, A., & McDermott, J. H. (2023). Model metamers reveal divergent invariances between biological and artificial neural networks. *Nature Neuroscience, 26*(11), 2017-2034.

[15] Chen, Z., Liang, Q., Wei, Z., Chen, X., Shi, Q., Yu, Z., & Sun, T. (2023). An overview of in vitro biological neural networks for robot intelligence. *Cyborg and Bionic Systems, 4*, 0001.

[16] Guest, O., & Martin, A. E. (2023). On logical inference over brains, behaviour, and artificial neural networks. *Computational Brain & Behavior, 6*(2), 213-227.

[17] Varley, T. F., Sporns, O., Schaffelhofer, S., Scherberger, H., & Dann, B. (2023). Information-processing dynamics in neural networks of macaque cerebral cortex reflect cognitive state and behavior. *Proceedings of the National Academy of Sciences, 120*(2), e2207677120.

[18] Chien, Y. C., Xiang, H., Shi, Y., Duong, N. T., Li, S., & Ang, K. W. (2023). A MoS2 Hafnium Oxide Based Ferroelectric Encoder for Temporal-Efficient Spiking Neural Network. *Advanced Materials, 35*(2), 2204949.

[19] Vijh, S., Saraswat, M., & Kumar, S. (2023). Automatic multilevel image thresholding segmentation using hybrid bio-inspired algorithm and artificial neural network for histopathology images. *Multimedia Tools and Applications, 82*(4), 4979-5010.

[20] Chen, H., Li, H., Ma, T., Han, S., & Zhao, Q. (2023). Biological function simulation in neuromorphic devices: from synapse and neuron to behavior. *Science and Technology of Advanced Materials, 24*(1), 2183712.